

# Very Low Temperature Tunnelling Spectroscopy in the heavy fermion superconductor $\text{PrOs}_4\text{Sb}_{12}$

H. Suderow,<sup>1</sup> S. Vieira,<sup>1</sup> J. D. Strand,<sup>2</sup> S. Bud'ko,<sup>2</sup> and P. C. Canfield<sup>2</sup>

<sup>1</sup>*Laboratorio de Bajas Temperaturas, Departamento de Física de la Materia Condensada  
Instituto de Ciencia de Materiales Nicolás Cabrera, Facultad de Ciencias  
Universidad Autónoma de Madrid, 28049 Madrid, Spain*

<sup>2</sup>*Ames Laboratory and Department of Physics and Astronomy  
Iowa State University, Ames, Iowa 50011, USA*

(Dated: October 31, 2018)

We present scanning tunnelling spectroscopy measurements on the heavy fermion superconductor  $\text{PrOs}_4\text{Sb}_{12}$ . Our results show that the superconducting gap opens over a large part of the Fermi surface. The deviations from isotropic BCS  $s$ -wave behavior are discussed in terms of a finite distribution of values of the superconducting gap.

PACS numbers: 74.70.Tx, 74.50.+r, 07.79.Cz

The intriguing magnetic and superconducting properties of most heavy fermion metals, which include e.g. coexistence of superconductivity with ferromagnetism, non-Fermi liquid behaviors or multiple superconducting phases, represent a challenge to our current understanding of condensed matter physics[1, 2, 3]. The route towards the discovery of new heavy fermions is to synthesize materials that maintain degrees of freedom (e.g. local magnetic or electric moments), which do not undergo a phase transition upon cooling and are coupled to the electron bath. A large entropy can then be preserved down to low temperatures, and transferred over to the electrons.  $\text{Pr}^{3+}$  ions offer this possibility if the Pr is in a cubic point symmetry, where the crystal electric field ground state can be a non-magnetic, non-Kramers  $\Gamma_3$  doublet, which can provide the entropy needed to create a heavy fermion ground state if a cooperative Jahn-Teller transition can be avoided[4, 5].  $\text{PrInAg}_2$  meets these criteria, and it was shown to be the first possible example of a Pr-based heavy fermion with a very large linear specific heat coefficient of  $6.5 \text{ J/mol K}^2$ [4]. Unfortunately  $\text{PrInAg}_2$  did not superconduct down to  $50\text{mK}$ , making it hard to independently ascertain that the large linear specific heat term was indeed of electronic origin. Recently superconductivity has been found with  $T_c=1.85\text{K}$  in another Pr based heavy fermion[6],  $\text{PrOs}_4\text{Sb}_{12}$ , where large electronic specific heat coefficients  $\gamma$  between  $300$  and  $500 \text{ mJ/mol K}^2$  have been reported[6, 7, 8, 9, 10]. The height of the jump of the specific heat at the superconducting transition, which compares well with BCS theory, shows that the large  $\gamma$  is indeed associated to the conduction electrons, and that, in addition, the heavy electronic bath superconducts [6, 7, 8, 9]. Moreover, two superconducting transitions have been clearly resolved in the specific heat at  $1.6$  and  $1.85 \text{ K}$  in high quality single crystalline samples, giving strong indications for the presence of multiple superconducting phases[7, 8, 9]. The situation seems analogous to the only other known stoichiometric superconductor that presents multiple superconducting phases,

$\text{UPt}_3$ [3, 11]. In that case, most present theoretical and experimental scenarios associate the Cooper pairing mechanism that leads to multiple phase superconductivity to magnetic fluctuations[11]. Instead, in  $\text{PrOs}_4\text{Sb}_{12}$ , interactions with fluctuating quadrupolar (electric) moments seem the most likely mechanism that drives the system to an unconventional, multiple phase superconducting state[6, 7, 8, 9, 10, 12, 13, 14]. Note also that the isostructural compound  $\text{LaOs}_4\text{Sb}_{12}$ , which does not show heavy fermion behavior[15], superconducts with a lower critical temperature ( $1\text{K}$  [8]).

The determination of the most fundamental superconducting properties of  $\text{PrOs}_4\text{Sb}_{12}$  is clearly needed to understand the formation of unconventional, multiple phase superconductivity. One of the first and most important points is to try to resolve the structure of the superconducting gap in the low temperature, low magnetic field phase, which occupies the largest part of the phase diagram[7]. Indirect information can be obtained by thermodynamic, transport, magnetic or NMR measurements, but the experiments that have been done up to now lead to contradictory results, and are therefore not conclusive. Specific heat does not seem adequate to study the superconducting gap, because it shows a high Schottky peak at low temperatures[6, 7, 8, 9, 10]. NQR measurements show an exponential decrease of  $1/T_1T$  at low temperatures[12] associated to a well developed gap. The London penetration depth, as measured with muon spin relaxation, also appears to decrease exponentially at low temperatures[13]. On the other hand, the angular dependent thermal conductivity under magnetic fields appears to be strongly modulated due to significant changes in the superconducting gap over the Fermi surface. This result has been associated to the presence of point nodes[14].

Here we present direct measurements of the superconducting gap in  $\text{PrOs}_4\text{Sb}_{12}$ , done with high resolution tunnelling spectroscopy studies in the superconducting phase with a Scanning Tunneling Microscope (STM). We find a superconducting density of states with no low energy

excitations and a well developed superconducting gap.

We use a home built STM unit and electronics installed in a partially home built dilution refrigerator. We have previously tested our experimental set-up by measuring the superconducting properties of Al, which is possibly the best known superconducting material with a critical temperature (1.2K) of the same order of magnitude as  $\text{PrOs}_4\text{Sb}_{12}$  (1.85K). The sharpest superconducting features that we could resolve up to now are the quasiparticle peaks shown in Fig.1a, where we represent the tunnelling spectroscopy when both tip and sample are of Al (prepared following [16]). The width of these features can be taken as a measure of the resolution in energy of our spectrometer, and therefore of the effective lowest temperature of our measurements. We find a width at half maximum of  $16\mu\text{V}$ , which corresponds to 184mK. On the other hand, the best fit to the tunnelling spectra taken between a normal tip of Au and a sample of Al (Fig.1b) using conventional isotropic BCS s-wave theory gives the same value for the temperature  $T=190\text{mK}$  (within the 5% uncertainty of the fit; we also use  $\Delta = 175\mu\text{eV}$ ). Therefore, we can take 190mK as the lowest measuring temperature that can be achieved at present with our set-up. Our resolution is similar to the one achieved in many planar junction experiments[17], with the important difference that in STM measurements the tunnelling current is between 4 to 6 orders of magnitude smaller.

Single crystals of  $\text{PrOs}_4\text{Sb}_{12}$  were grown out of a ternary melt that was rich in both Os and Sb. A starting composition of  $\text{Pr}_2\text{Os}_{16}\text{Sb}_{82}$  was heated to 1200 °C and cooled over 100 hours to 725 °C and then decanted, revealing small cubic crystals. We measured three samples in eight different cool downs by placing an Au tip on optically neat and flat faces of the single crystals. Within a given cool down, we changed the macroscopic position of the Au tip on the surface and measured many (more than 50 in total) different scanning windows ( $100\times 100\text{nm}^2$ ), using the positioning capabilities of our xy table, as in previous work [18]. The measured work functions were always of several eV and the topography was reproducible upon changes of the tunnelling current. It consists of inclined planes and bumps, with typical corrugations of about 4nm (inset of Fig.2), indicating that the crystallographic direction of the surface is not well defined at the nanoscopic length scales relevant for this experiment.

Typical spectra (Fig.2) show a clean density of states with no low energy excitations, demonstrating that the superconducting gap is well developed over a large part of the Fermi surface. The best fit with isotropic BCS s-wave theory is shown by the line in Fig.2. Using  $T=0.19\text{K}$  we obtain a value for the superconducting gap  $\Delta=270\mu\text{eV}$ , which gives  $2\Delta/k_B T_c=3.4$ , very close to the BCS value 3.53. Note that differences between the experiment and the fit are clearly resolved thanks to the high resolution in voltage of our experiment, evidenced by the curves shown in Fig.1.

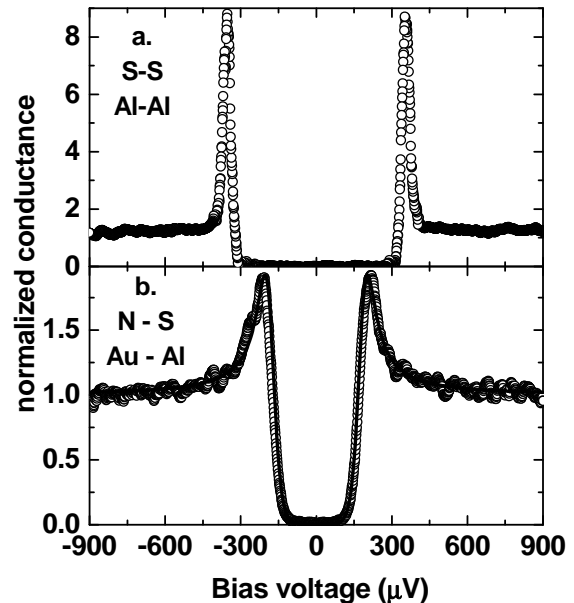


FIG. 1: In a. we show the tunnelling conductance measured at the lowest temperatures of our set-up, normalized to its value at high voltages (the tunnelling resistance in this and all subsequent figures is  $1\text{M}\Omega$ ) when both tip and sample are of Al. The preparation procedure is the same as in [16]. The peak is the sharpest superconducting feature that we could resolve with our experiment and it gives a measure of the resolution of our spectrometer (184 mK, see text). The tunnelling conductance between an Au tip and a sample of Al (b.), taken also at the lowest temperatures, gives an excellent fit with isotropic, BCS s-wave theory if we take  $T=0.19\text{K}$  and  $\Delta=175\mu\text{eV}$  (line in b.).

The tunnelling current depends on the overlap of the electron wavefunctions of tip and sample near the surface, being therefore a sum of the contributions from electrons coming from different sheets of the Fermi surface having  $k$ -vectors with different orientations. If the superconducting gap is anisotropic in a given sheet, or it has different values in different sheets of the Fermi surface, or both, the tunnelling spectra reflect this distribution of values of the superconducting gap by showing more broadened coherence peaks, which produce a deviation from isotropic BCS s-wave behavior (Fig.2 and e.g. Ref.[19]). Note that the presence of defects, grain boundaries or other perturbations that one can figure out to occur near the surface, can lead either to a decrease of the observed anisotropy through the mixing of the electronic wavefunctions from different parts of the Fermi surface caused by strong inter and/or intraband electronic scattering[20, 21, 22, 23], or to pair breaking. The former was not observed, and the latter always leads to an increased residual density of states at the Fermi level, which we can indeed observe in some locations of the surface, as discussed further on. Therefore, we believe that the deviations between the ex-

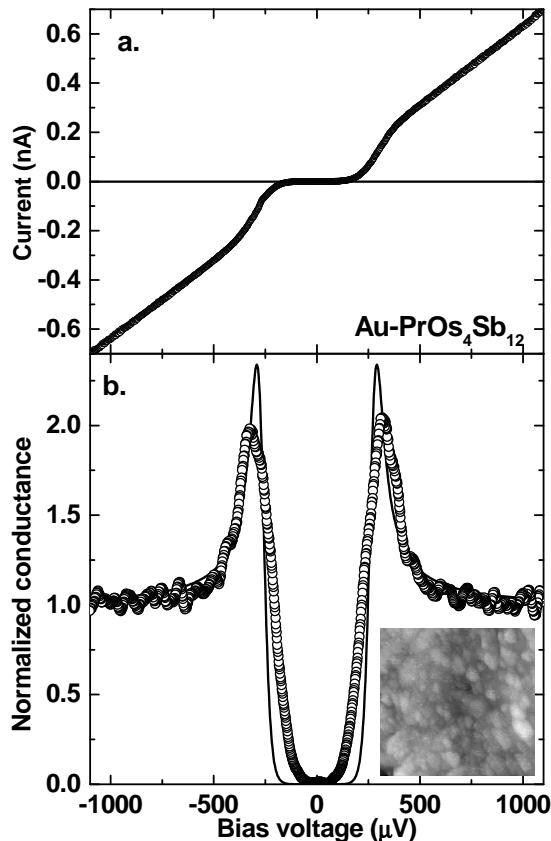


FIG. 2: Current-voltage characteristics (a) and tunnelling conductance (b.) of  $\text{PrOs}_4\text{Sb}_{12}$  at 0.19K. The superconducting gap is well developed with no low energy excitations. The line in b is the prediction from conventional isotropic BCS s-wave theory using  $\Delta = 270\mu\text{V}$  and  $T=0.19\text{K}$ . The inset in b shows a typical topographic image of the surface, representing an area of  $50\text{nm}\times 50\text{nm}$ , which shows a corrugation of about 4 nm.

periment and the fit shown in Fig.2 are intrinsic to the superconducting density of states in this compound.

Note that the conductance begins to increase at about  $120\mu\text{V}$ , and the highest point of the coherence peak is located at  $325\mu\text{V}$ . As a matter of fact, the shape of the tunnelling spectra we find is similar to the form of the spectra taken in the much studied material  $\text{NbSe}_2$ [19], where first experiments clearly showed up the presence of a distribution of values of the superconducting gap over the Fermi surface[19]. Subsequent work has identified this distribution as coming from different gap values in different sheets of the Fermi surface in that compound (multiband superconductivity)[24, 25]. Whereas more work is clearly needed to understand the origin of the gap distribution in  $\text{PrOs}_4\text{Sb}_{12}$ , it is noteworthy to remark that strong changes in the mass renormalization in different sheets has been found in the de Haas van Alphen experiments of Ref.[15]. These changes may also lead to the distribution of values of the superconducting

gap measured in our experiment. This strengthens both the idea that the mass renormalization and superconductivity are of the same origin, i.e. that the quadrupolar fluctuations favor superconducting correlations, as well as the possible multiband character of superconductivity in this compound.

The spectra are smeared when we increase the temperature, as shown in Fig.3a, and become flat above the bulk critical temperature (1.85K). The maximum in the derivative of the conductance within the quasiparticle peaks, which gives a good estimate of the mean value of the superconducting gap [22] is shown in Fig.3b and it follows well the temperature dependence of the superconducting gap within BCS s-wave theory (line in Fig.3b). The curve can be extrapolated to a critical temperature of 1.8K, which is the bulk  $T_c$  (1.85K) value within our experimental error (10%).

The superconducting properties in this compound clearly differ from the ones in magnetically mediated Ce or U heavy fermions. Although we could not find any published STM measurements in the tunnelling regime and in the superconducting phase in these materials, there is compelling evidence from many different techniques sensitive to the superconducting density of states that a large amount of low energy excitations due to a strongly anisotropic superconducting gap is found in most cases. For instance, many experiments show now that the multiphase superconductor  $\text{UPt}_3$  presents a line node along the basal plane and nodes along the c axis of its hexagonal crystalline structure, with a superconducting gap that decreases by more than an order of magnitude at the nodes [11, 26]. In the case of  $\text{PrOs}_4\text{Sb}_{12}$ , there are at present no data pointing towards extended gapless regions on the Fermi surface, as the one caused by a line of nodes, so that the superconducting gap appears to be opened in a much larger part of the Fermi surface than in  $\text{UPt}_3$ .

The observed behavior has been reproduced in different places, but it is not found over the whole surface. In general, regions with no residual density of states, as shown in Fig.4 a and b, have typical sizes of several times the coherence length ( $\xi_0=12\text{nm}$ [6]) and are surrounded by regions where a finite density of states appears at the Fermi level, shown in Fig.4 c and d. We can also easily find regions with much less well defined superconducting features (not shown in the figure). When we find a finite density of states at the Fermi level, the superconducting features also disappear at a temperature smaller than critical temperature of the bulk, indicating that the physical origin for the residual density of states at the Fermi level is some kind of strong pair breaking effect appearing near the surface, easily detected with our technique.

In conclusion, we performed a direct measurement of the superconducting gap through high resolution local tunnelling spectroscopy measurements in the heavy fermion superconductor  $\text{PrOs}_4\text{Sb}_{12}$ . Typical spectra

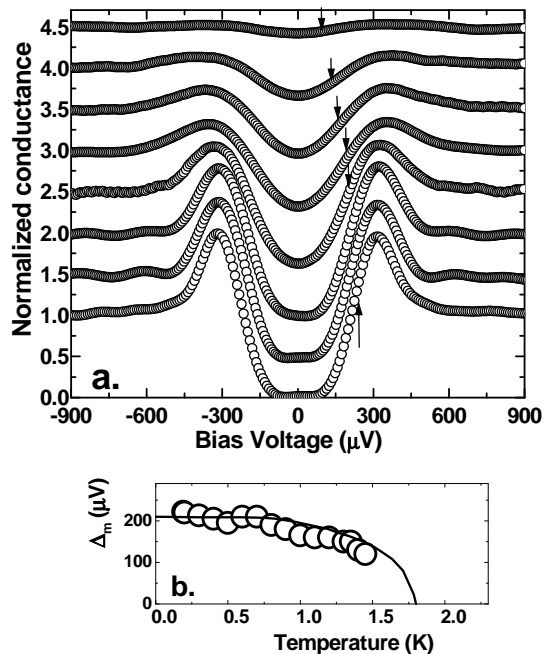


FIG. 3: in a. we show the temperature dependence of the tunnelling conductance. The curves have been displaced by 0.5 units in the y axis for clarity. The data were taken at 0.2,0.3,0.4,0.6,0.8,1,1.2,1.4 K from bottom to top. In b., the temperature dependence of the maximum in the derivative of the conductance is shown (also with arrows in a.). This gives a good estimation of the mean value of the superconducting gap and it fits well to BCS theory (line). The extrapolated critical temperature coincides with the value found in the bulk.

demonstrate that the superconducting gap is well developed over a large part of the Fermi surface. The presence of a finite distribution of values of the superconducting gap over the Fermi surface can be inferred from deviations between the experiment and isotropic BCS s-wave behavior.

We acknowledge discussions with J.P. Brison, M. Crespo, J. Flouquet, F. Guinea, K. Izawa Y. Kitaoka, A. Levanyuk and J.G. Rodrigo and support from the ESF programme VORTEX, from the MCyT (Spain; grant MAT-2001-1281-C02-0), and from the Comunidad Autónoma de Madrid (07N/0053/2002, Spain). The Laboratorio de Bajas Temperaturas is associated to the ICMM of the CSIC. Ames Laboratory is operated for the U. S. Department of Energy by Iowa State University under Contract No. W-7405-Eng-82. This work was supported by the Director for Energy Research, Office of Basic Energy Sciences.

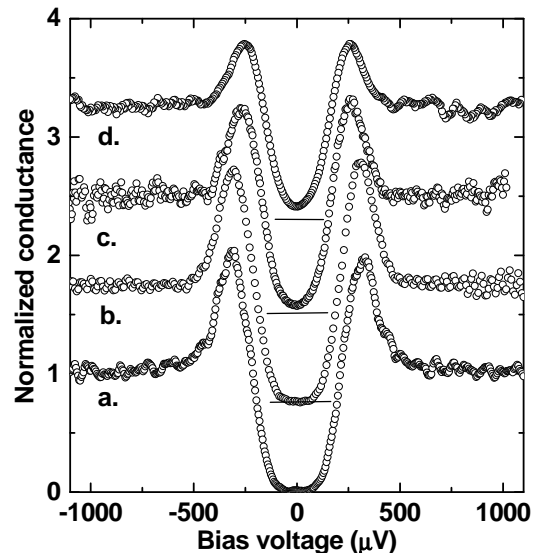


FIG. 4: Set of tunnelling conductance curves taken in different positions on the surface of  $\text{PrOs}_4\text{Sb}_{12}$  at 0.19K. The curves have been displaced by 0.75 units in the y axis for clarity, and the lines show the location of zero conductance for each curve. The finite density of states at the Fermi level measured in some positions (c and d) shows that pair breaking effects can appear at the surface of this compound.

[1] A.D. Hewson, *The Kondo problem to heavy fermions* (Cambridge University Press, Cambridge, England 1993).

- [2] D. Aoki *et al.* *Nature*, **413**, 613-616 (2001).  
 [3] K. Hasselbach, L. Taillefer, J. Flouquet, *Phys. Rev. Lett.* **63**, p. 93 (1989); R.A. Fisher *et al.*, *Phys. Rev. Lett.* **62**, 1411 (1989).  
 [4] A. Yatskar *et al.* *Phys. Rev. Lett.* **77**, 3637-3640 (1996)  
 [5] D.L. Cox, *Phys. Rev. Lett.* **59**, 1240 (1987)  
 [6] E.D. Bauer *et al.*, *Phys. Rev. B*, **65**, 100506(R), 2002.  
 [7] R. Vollmer *et al.* *Phys. Rev. Lett.* **90**, 057001 (2003).  
 [8] M.B. Maple, *Acta Physica Polonica B v.* **34**, 919 (2003), cond-mat/0303370.  
 [9] M.A. Measson *et al.*, to be published.  
 [10] Y. Aoki *et al.*, *J. Phys. Soc. of Japan* **71**, 2098, (2002).  
 [11] R. Joynt, L. Taillefer, *Rev. of Mod. Phys.* **74**, 235-294 (2002)  
 [12] H. Kotegawa *et al.* *Phys. Rev. Lett.* **90**, 027001 (2002).  
 [13] D.E. MacLaughlin *et al.* *Phys. Rev. Lett.* **89**, 157001 (2002).  
 [14] K. Izawa *et al.* *Phys. Rev. Lett.* **90**, 117001 (2003).  
 [15] H. Sugawara *et al.*, *Phys. Rev. B* **66**, 220504 (2002).  
 [16] H. Suderow *et al.*, *Phys. Rev. B* **65**, R100519 (2002), and references therein.  
 [17] E.L. Wolf, "Principles of Electron Tunnelling Spectroscopy", Oxford University Press (1989).  
 [18] G. Rubio-Bollinger, H. Suderow, S. Vieira, *Phys. Rev. Lett.* **86**, 5582 (2001).  
 [19] H.F. Hess, R.B. Robinson, and J.V. Waszczak, *Phys. Rev. Lett.* **64**, 2711 (1990).  
 [20] C.C. Sung, V.K. Wong, *J. Phys. Chem. Solids*, **28**, 1933 (1967).  
 [21] A. A. Golubov and I. I. Mazin, *Phys. Rev. B* **55**, 15146-15152 (1997)  
 [22] P. Martinez-Samper *et al.*, *Physica C* **385**, 233 (2003).  
 [23] P. Martinez-Samper *et al.*, *Physical Review B* **67**, 014526

- (2003).
- [24] E. Boaknin, et al. Phys. Rev. Lett. **90**, 117003 (2003)
- [25] T. Yokoya et al., Science **294**, 2518 (2001).
- [26] See also e.g. H. Suderow et al. Phys. Rev. Lett. **80**, 165 (1998).